Supporting Information

Small-molecule/fullerene acceptor alloy: A powerful tool to enhance device efficiency and thermal stability of ternary polymer solar cells

Pan Yin[a], Linqiao Wang[a], Jingtang Liang[a], Yufu Yu[a], Li Chen[a], Chao Weng[a], Chaohua Cui,[b] and Ping Shen[a]*

[a] Key Laboratory for Green Organic Synthesis and Application of Hunan Province, Key Laboratory of Environmentally Friendly Chemistry and Application of Ministry of Education, College of Chemistry, Xiangtan University, Xiangtan 411105, China

E-mail: shenping802002@163.com

[b] Laboratory of Advanced Optoelectronic Materials, College of Chemistry, Chemical Engineering and Materials Science, Soochow University, Suzhou 215123, China

Experimental section

Analytical instruments

Nuclear magnetic resonance (NMR) spectra were measured with Bruker AVANCE 400 spectrometer. Ultraviolet-visible (UV-vis) absorption spectra were measured on PerkinElmer Lamada 25 spectrometer. The photoluminescence (PL) spectrum was conducted on an Edinburgh Instrument FLS 980. Molecular mass was determined by flight mass spectrometry (MALDITOF MS) using a Bruker Aupoflex-III mass spectrometer. Thermal gravimetric analysis (TGA) was performed under nitrogen at a heating rate of 20 °C min^{-1} with TGA Q50 analyzer. Differential scanning calorimetry (DSC) analysis was conducted on a DSC instrument (DSC Q10) under N_2 with a heating rate of 5 °C min^{-1}. The electrochemical cyclic voltammetry (CV) was recorded on a electrochemistry work station (CHI830B, Chenhua Shanghai) with a Pt slice electrode (coated with a polymer film), a Pt ring, and an Ag/AgCl electrode as the working electrode, the auxiliary electrode and the reference electrode respectively, in a 0.1 mol L^{-1} tetrabutylammonium hexafluorophosphate (Bu$_4$NPF$_6$) acetonitrile

solution. The HOMO/LUMO energy levels were gained from the equation HOMO/LUMO = -$(E_{ox/red}^{onset} - E_{Fc/Fc+} + 4.8)$ (eV), where $E_{ox/red}^{onset}$ refers the onset oxidation/reduction potential and the redox potential ($E_{Fc/Fc+}$) of Fc/Fc$^+$ was determined to be 0.45 V versus Ag/AgCl in this measurement system. Therefore, the above equation can be simplified to be HOMO/LUMO = -$(E_{ox/red}^{onset} + 4.35)$ (eV). Atomic force microscopy (AFM) measurement was carried out on a Digital Instruments Veeco Nanoscopy V using a tapping mode. Transmission electron microscopy (TEM) were performed on a JEM-2100 electron microscope operating at an acceleration voltage of 100 Kv.

Materials

Toluene and tetrahydrofuran (THF) were refluxed and distilled from sodium with benzophenone as an indicator prior to use. *N*, *N'*-Dimethylformamide (DMF) was distilled after drying by CaH$_2$. *n*-Butyllithium (*n*-BuLi, 2.5 M in THF), 3,4-dimethoxythiophene, 1-bromo-4-(hexyloxy)benzene, 3-(dicyanomethylene)indian-1-one, trimethyltin chloride, 2,5-dibromoterephthalic acid diethyl ester and Pd(PPh$_3$)$_4$ were purchased from Energy Chemical. The polymer donor PBDB-T and PC$_{71}$BM were commercially obtained from Derthon (Shenzhen China) Optoelectronic Materials Science Technology Co., Ltd. Intermediate **M2** was synthesized according to the previously reported procedure.[1]

Synthesis of the Small-Molecule Acceptor IDT-OT

The synthetic route of the target SMA of IDT-OT was presented as **Scheme S1**. The synthetic details of intermediates and target molecule were showed as follows.
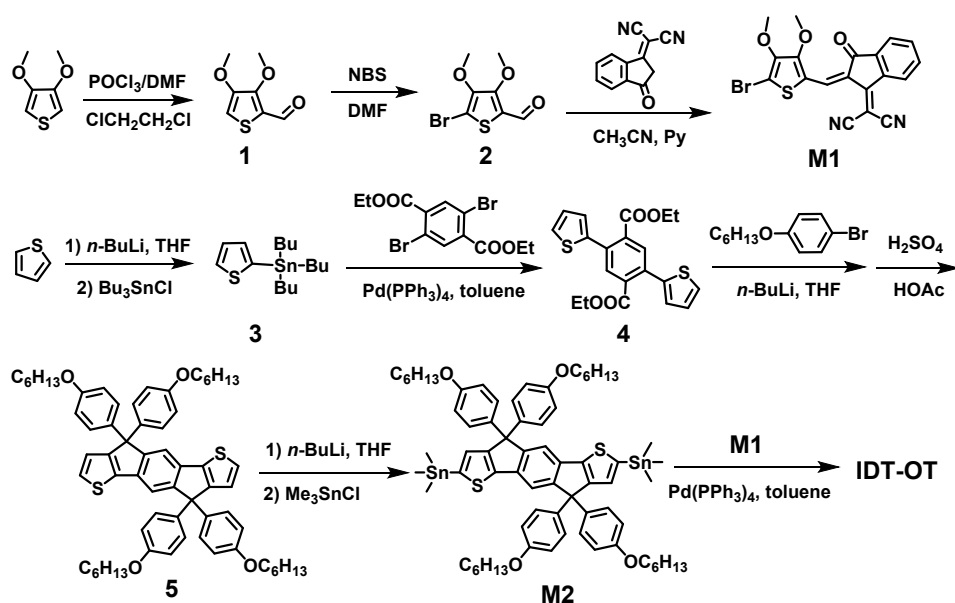
Scheme S1. The synthetic route of IDT-OT.

Synthesis of 3,4-dimethoxylthiophene-2-carbaldehyde (compound 1)

To a dry 100 mL three-necked round bottom flask, 3,4-dimethoxythiophene (1.4 g, 10.0 mmol), 2.3 mL dried DMF and 20 mL 1,2-dichloroethane were added under a nitrogen atmosphere. The solution was cooled to 0 °C and stirred when 2.8 mL of phosphoryl chloride was added dropwise. The mixture was stirred for 0.5 h at 0 °C and continually stirred at 90 °C for another 4 h. After cooling to room temperature, the mixture was poured into 20 mL of 1 M NaOH solution and extracted with dichloromethane for three times. The combined organic phase was washed with brine three times and dried over anhydrous $MgSO_4$. Finally, the crude product was purified via silica gel column chromatography with petroleum ether/dichloromethane (1:10, by volume) as eluent to afford compound **1** as a white solid (1.3 g, yield 75%). ^{1}H NMR (400 MHz, $CDCl_3$, δ/ppm): 10.02 (s, 1H), 6.65 (s, 1H), 4.12 (s, 3H), 3.87 (s, 3H).

Synthesis of 5-bromo-3,4-dimethoxylthiophene-2-carbaldehyde (compound 2)

To a dry 100 mL three-necked round bottom flask, compound **1** (1.3 g, 7.5 mmol) and 5 mL DMF were added under a nitrogen atmosphere. The solution was cooled to 0 °C and stirred when NBS (1.5 g, 8.3 mmol) dissolved in 15 mL DMF was added dropwise. The mixture was stirred for 0.5 h at 0 °C and then warmed up to room temperature to stir for another 12 h. The mixture was poured into 50 mL water and extracted with dichloromethane for three times. The combined organic phase was washed with brine three times and dried over anhydrous $MgSO_4$. Finally, the crude product was purified via silica gel column chromatography with petroleum ether/dichloromethane (1:1, by volume) as eluent to afford compound **2** as a yellow solid (1.0 g, yield 53%). ^{1}H NMR (400 MHz, $CDCl_3$, δ/ppm): 9.91 (s, 1H), 4.13 (s, 3H), 3.92 (s, 3H).

*Synthesis of intermediate **M1***

To a dry 100 mL three-necked round bottom flask, compound **2** (1.3 g, 5.0 mmol), 1,1-(dicyanomethylene)-3-indanone (1.0 g, 5.0 mmol), 30 mL acetonitrile and 0.1 mL piperidine were added under argon atmosphere. The reaction mixture was stirred at 85 °C for 5 h. After cooling to room temperature, the crude product was purified via silica gel column chromatography with petroleum ether/dichloromethane (1:1, by volume) to afford the intermediate **M1** as a red solid (1.4 g, yield 66%). ^{1}H NMR (400 MHz, $CDCl_3$, δ/ppm): 9.10 (s, 1H), 8.69 (d, J = 8.0 Hz, 1H), 7.92 (d, J = 8.0 Hz, 1H), 7.78-7.74 (m, 2H), 4.16 (s, 3H), 3.96 (s, 3H).

*Synthesis of target SMA **IDT-OT***

To 100 mL three-necked round bottom flask, **M1** (769 mg, 1.8 mmol), **M2** (780 mg, 0.6 mmol) and toluene (35 mL) were added and degassed for 30 min under a nitrogen atmosphere before $Pd(PPh_3)_4$ (50.0 mg, 7% mmol) was added quickly. The reaction mixture was stirred at 110 °C for 24 h. After cooling to room temperature, water (50 mL) was added into the reaction mixture and then it was extracted with CH_2Cl_2 (3 × 50 mL). The combined organic phases were washed with brine three times and dried over anhydrous $MgSO_4$. Finally, the crude product was purified via silica gel column chromatography with petroleum ether/dichloromethane (1:1, by volume) as eluent to afford the target small molecule **IDT-OT** as a red-black solid (450 mg, yield 47%). ^1H NMR (400 MHz, CDCl$_3$, δ/ppm): 9.11 (s, 2H), 8.66 (d, J = 8.0 Hz, 2H), 7.87-7.85 (m, 2H), 7.72-7.68 (m, 4H), 7.55 (s, 2H), 7.49 (s, 2H), 7.20 (d, J = 8.0 Hz, 8H), 6.84 (d, J = 12.0 Hz, 8H), 4.17 (s, 6H), 3.97 (s, 6H), 3.93 (t, J = 8.0 Hz, 8H), 1.79-1.72 (m, 8H), 1.45-1.42 (m, 8H), 1.33-1.31 (m, 16H), 0.88 (t, J = 6.0 Hz, 12H); ^{13}C NMR (100 MHz, CDCl$_3$, δ/ppm): 188.85, 160.72, 160.44, 158.33, 157.56, 155.04, 146.76, 144.82, 140.22, 139.13, 136.70, 136.37, 135.76, 135.65, 134.90, 134.11, 132.52, 129.03, 125.16, 123.44, 122.70, 120.37, 118.75, 117.90, 115.11, 114.91, 114.47, 77.36, 77.25, 77.04, 76.72, 68.13, 68.03, 62.28, 61.88, 60.59, 31.59, 29.25, 25.76, 22.62, 14.05; MS (MALDI-TOF, *m/z*) calcd. for $C_{102}H_{94}O_{10}S_4$: 1664.132, found 1664.952.

PSC Device Preparation and Performance Test

The devices with an inverted structure of ITO/ZnO/active layer/MoO$_3$/Al were fabricated and characterized in an N$_2$-filled glovebox, where the active layer was of the binary or ternary blends comprised with polymer donor PBDB-T, PC$_{71}$BM and/or IDT-OT. The indium tin oxide (ITO) patterned glass was cleaned with ultrasonic treatment in detergent, deionized water, acetone, ethanol, and isopropyl alcohol sequentially, and dried in an ultraviolet–ozone chamber for 15 min. The ZnO layer was deposited by spin-coating on top of a pre-cleaned ITO-coated glass substrate. And then, the active layer was spin-coated on the ZnO layer from a blend solution. The binary and ternary blends were dissolved in chlorobenzene (CB) with different weight ratios. The total concentration of the donor and acceptor materials was kept 20 mg mL^{-1}. The device was transferred to a glove box, where the above prepared blend solution was then spin-coated on ZnO surface as the active layer. Here, it should be noted that a certain amount of 1,8-diiodooctane (DIO) was added to use as a process additive if

necessary. Subsequently, a MoO$_3$ layer (~10 nm) and an Al layer (~100 nm) were evaporated though a shadow mask and form a top anode. The active area of the devices was defined as about 0.04 cm^2 by a shadow mask. The thicknesses of the active layer was determined to be ~ 100 nm by measuring on an Ambios Technology XP-2 surface profilometer. Photovoltaic performance of solar cells was tested under illumination condition with an AM 1.5G (100 mW cm^{-2}), and the current density-voltage (*J-V*) characteristics were measured by a computer controlled Keithley 2450 Source Meter. The EQE was measured by using a Solar Cell Spectral Response Measurement System QE-R3011 (Enli Technology Co., Ltd.). The light intensity at each wavelength was calibrated by a standard single-crystal Si solar cell.

The charge mobility was measured by the space charge-limited current (SCLC) method with a hole-only device configuration (ITO/PEDOT:PSS/active layer/MoO$_3$/Al) for hole mobility and an electron-only device configuration (ITO/ZnO/active layer/Ca/Al) for electron mobility. Both hole and electron mobilities were extracted by fitting measured *J-V* curves using the empirical Mott–Gurney formula in single carrier SCLC device with the equation of $ln(JL^3/V^2) \approx 0.89(1/E_0)^{0.5} (V/L) + ln(9\varepsilon_0\varepsilon_r\mu/8)$.
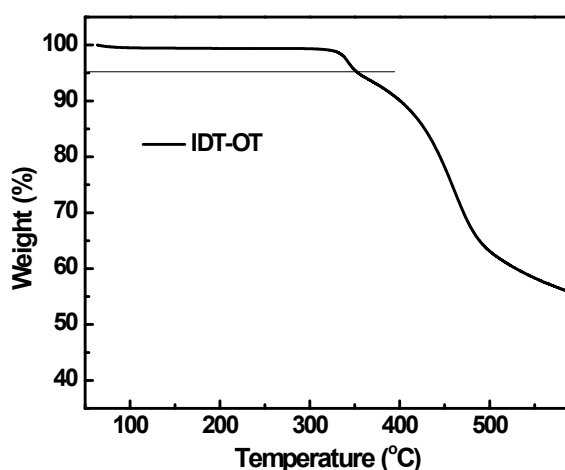

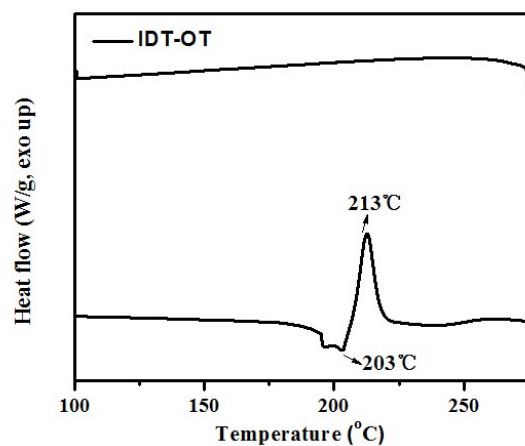**Fig. S1** TGA curve of IDT-OT under nitrogen atmosphere at a heating rate of 20 °C min^{-1}.

Fig. S2 DSC curve of IDT-OT under nitrogen atmosphere at a heating rate of 5 °C min^{-1}.
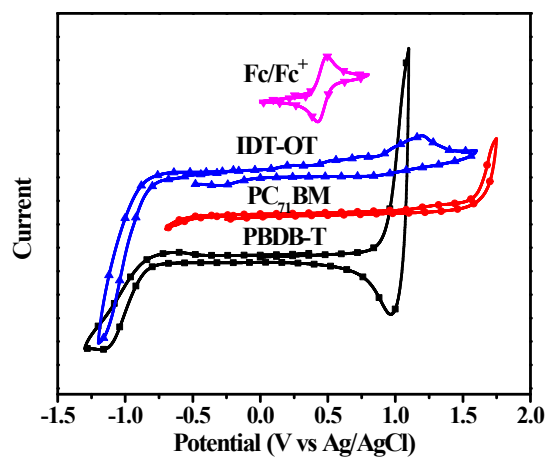

Fig. S3 Cyclic voltammograms of the polymer donor PBDB-T, SMA IDT-OT, and PC$_{71}$BM films on platinum electrode in acetonitrile solution containing 0.1 mol L^{-1} Bu$_4$NPF$_6$ at a scan rate of 0.1 V s^{-1}.
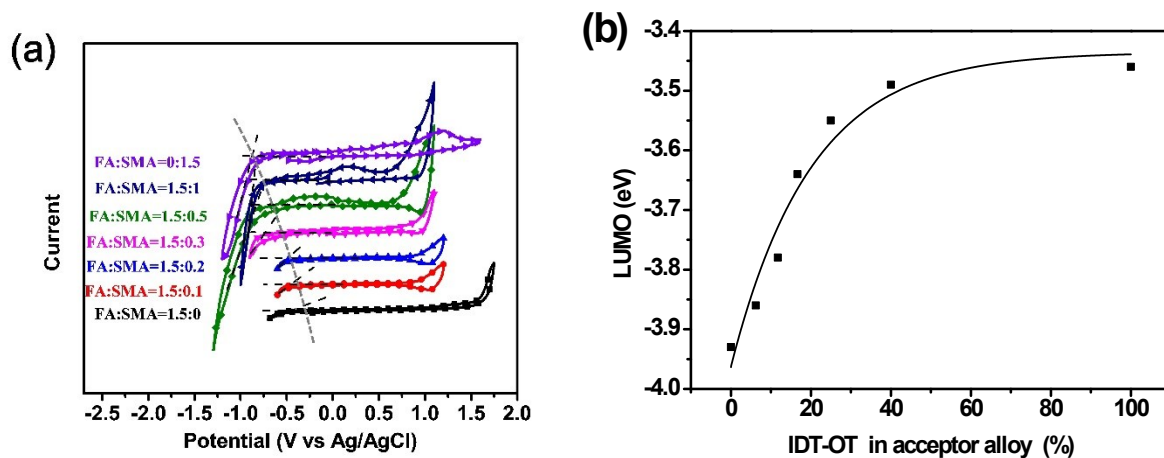
Fig. S4 (a) Cyclic voltammograms of the acceptor blend; (b) Measured LUMO level of the PC$_{71}$BM/IDT-OT blend as a function of the proportion of IDT-OT in acceptor alloy.
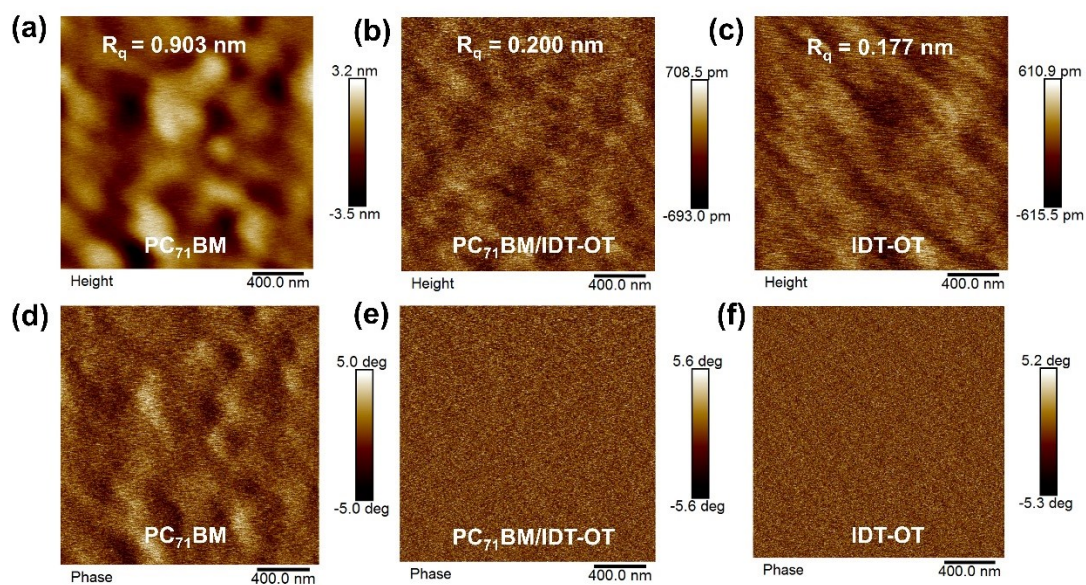

Fig. S5 a-c) AFM height images and d-f) phase images of the pristine PC$_{71}$BM film, P PC$_{71}$BM/IDT-OT blend film and pristine IDT-OT film.

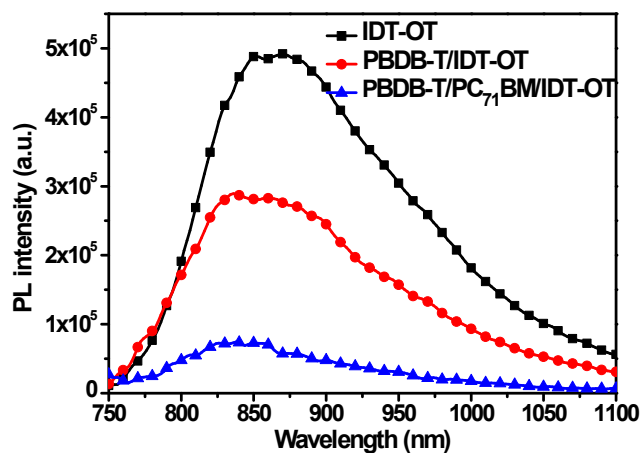**Fig. S6** PL spectra of the pure IDT-OT film, binary PBDT-T/IDT-OT and ternary PBDB-T/PC$_{71}$BM/IDT-OT (1:1.5:0.2) blend films excited at 750 nm.
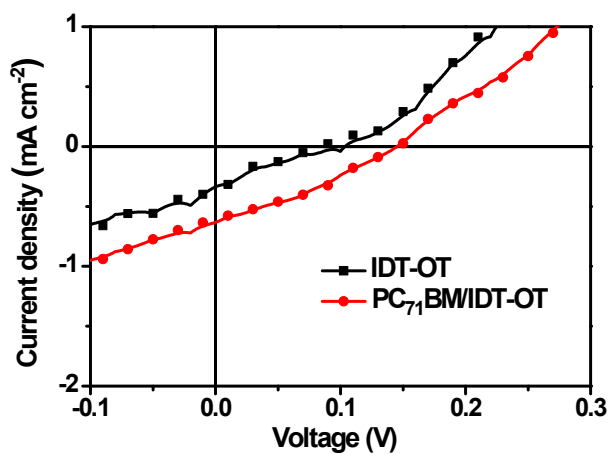
Fig. S7 The *J-V* plots of donor-free devices based on IDT-OT and PC$_{71}$BM/IDT-OT system.
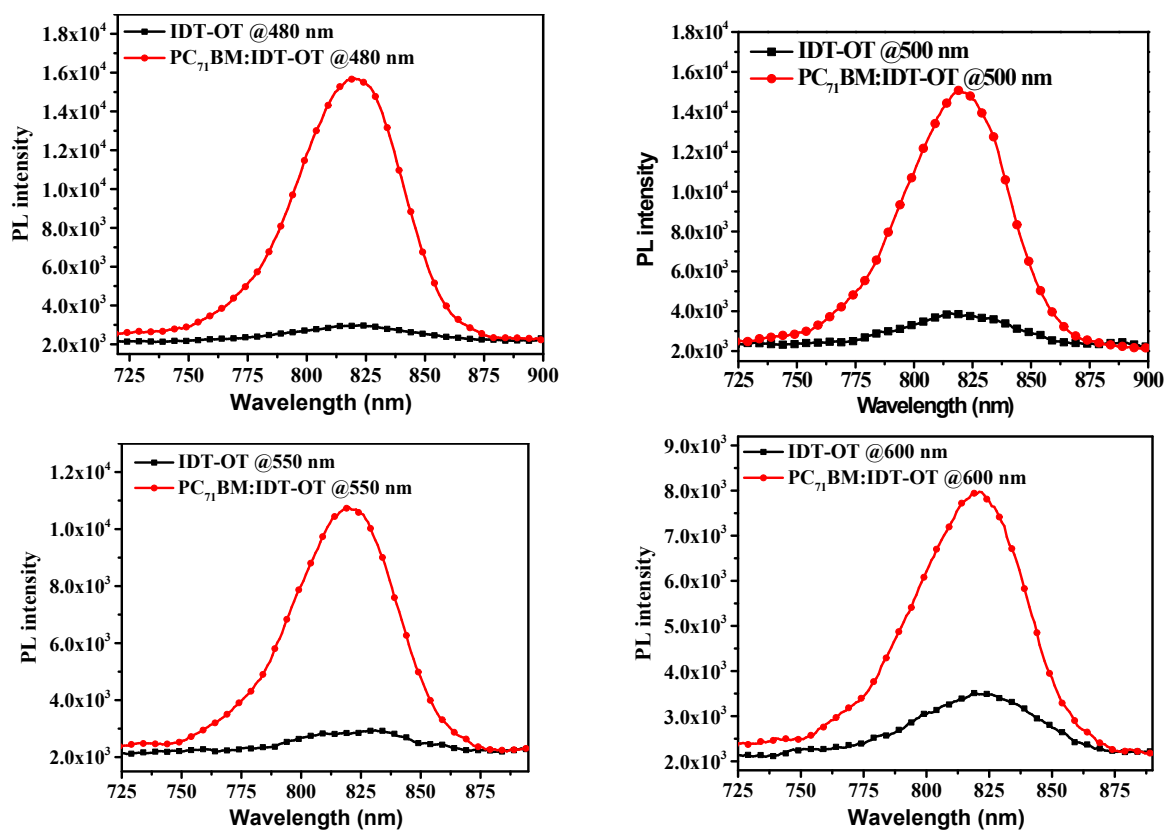
Fig. S8 PL spectra of the IDT-OT and binary PC$_{71}$BM/IDT-OT (1.5:0.2) blend films excited at different excited wavelength (480, 500nm, 550, and 600 nm).
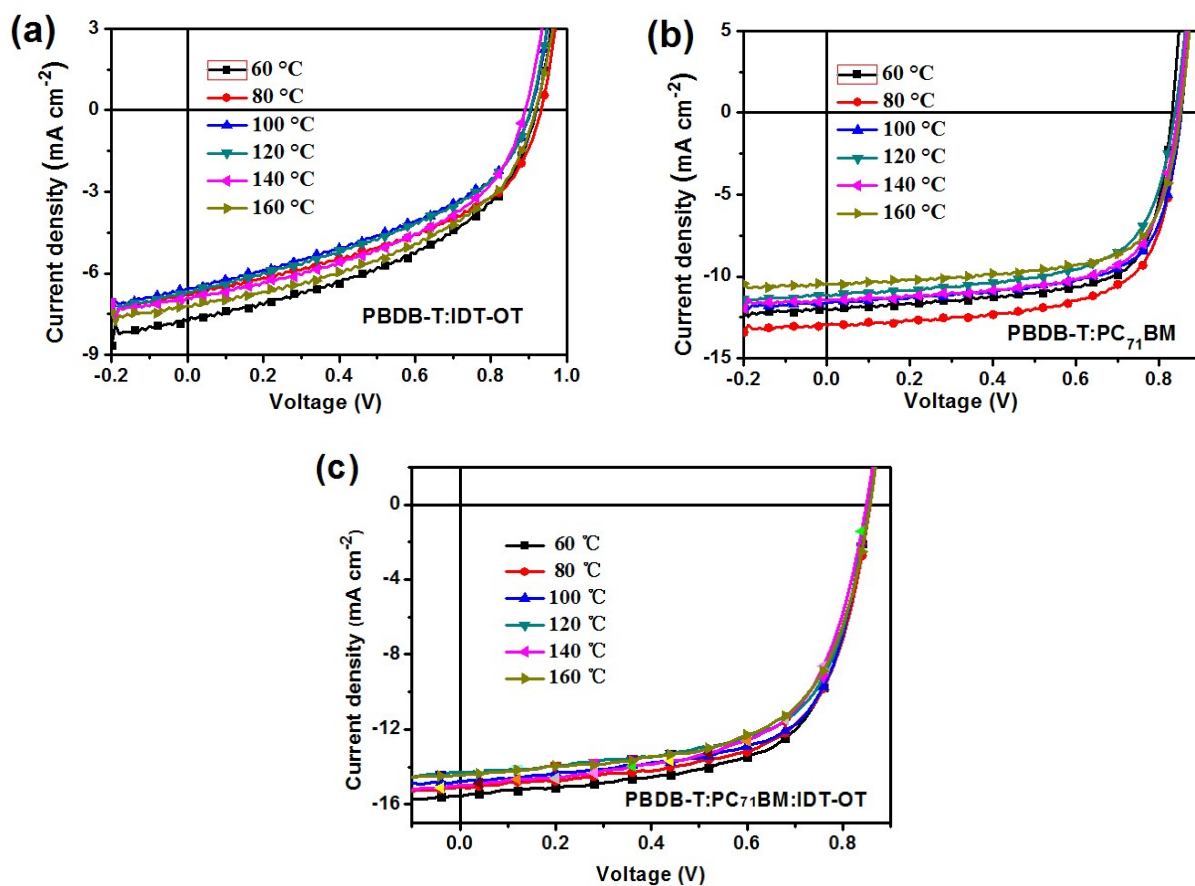
Fig. S9 The *J-V* plots of the binary and ternary devices with different annealing temperatures: (a) PBDB-T/IDT-OT, (b) PBDB-T/PC$_{71}$BM, and (c) PBDB-T/PC$_{71}$BM/IDT-OT.

Fig. S10 The AFM height and phase images of the ternary blend film under various thermal treatment conditions (60 °C, 100 °C, and 120 °C).

Fig. S11 The *J-V* plots of the binary and ternary devices with different annealing time at 120 °C under the optimal fabricated conditions: (a) PBDB-T/IDT-OT, (b) PBDB-T/PC$_{71}$BM, and (c) PBDB-T/PC$_{71}$BM/IDT-OT.

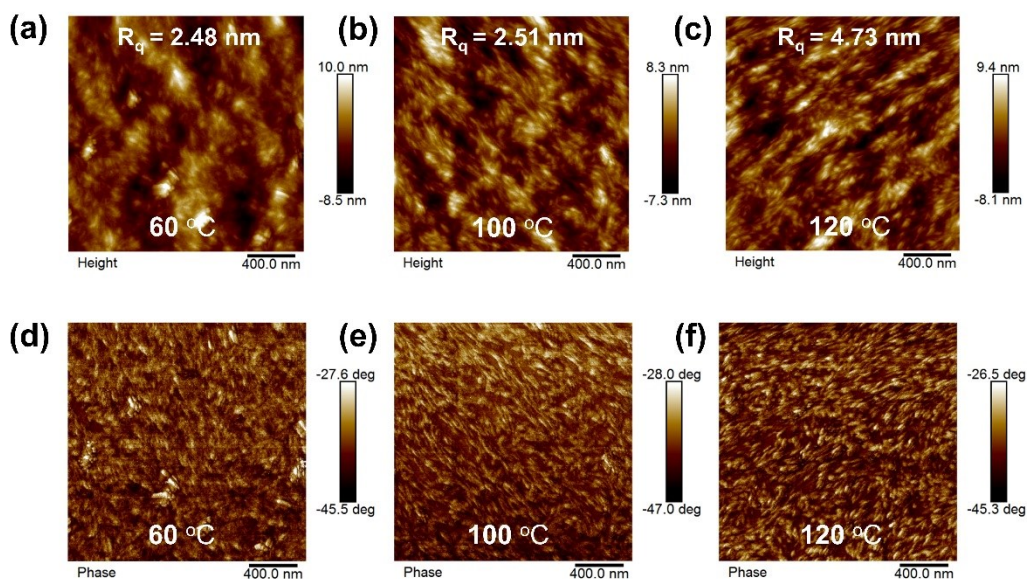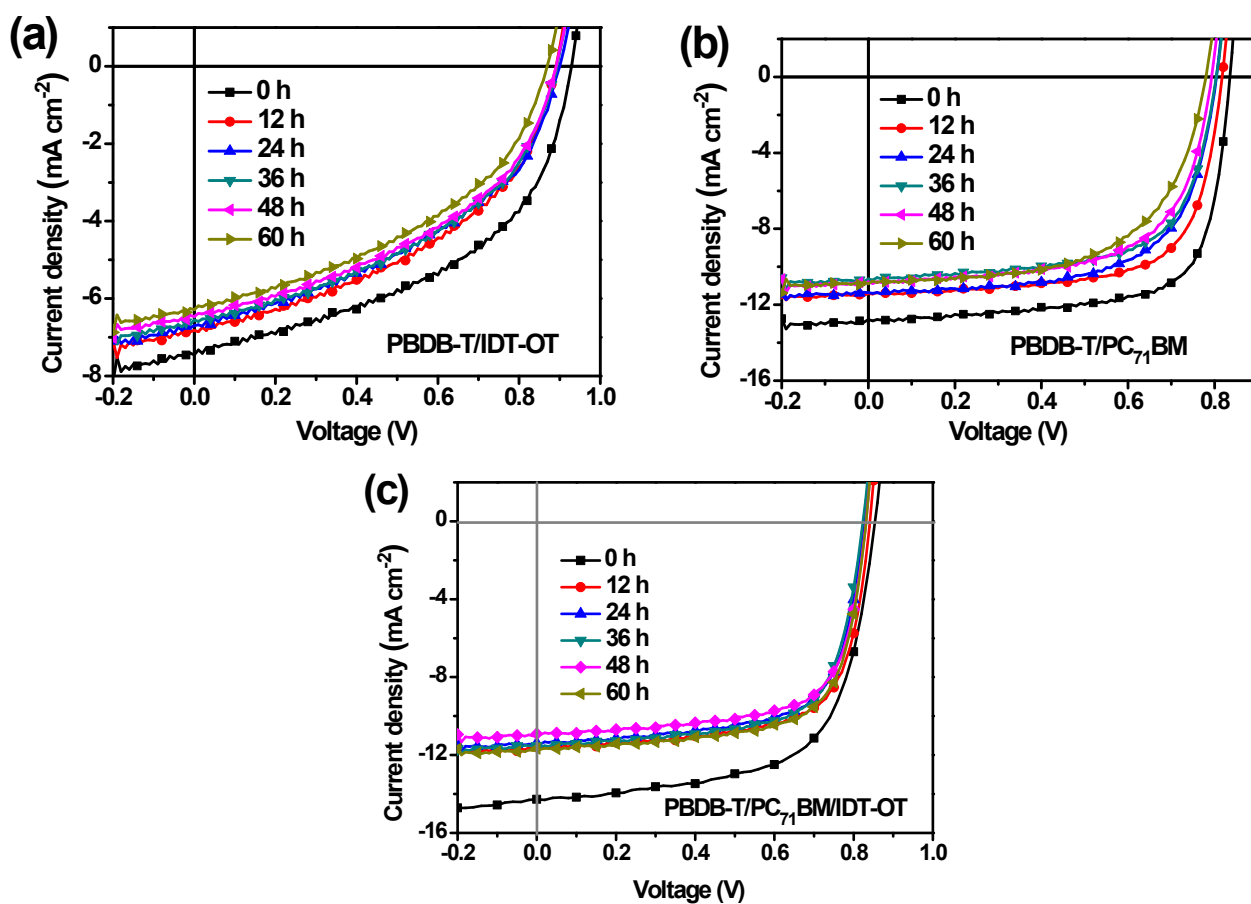**Table S1** Photovoltaic performance of the host PBDB-T/PC$_{71}$BM binary PSCs with different fabricated conditions. The devices were in inverted structure of ITO/ZnO/active layer/MoO$_3$/Al.

PBDB-T/PC$_{71}$BM [weight ratio]	V_{oc} [V]	J_{sc} [mA cm^{-2}]	FF [%]	PCE [%]	DIO [vol%]
1:1	0.89	10.28	64.1	5.90	0
1:1.5	0.89	11.40	68.7	6.98	0
1:2	0.88	11.53	61.1	6.22	0
1:1.5	0.82	14.50	58.0	6.92	1
1:1.5	0.826	14.10	66.8	7.78	3

Table S2 Photovoltaic performance of the reference PBDB-T/IDT-OT binary PSCs with different fabricated conditions. The devices were in inverted structure of ITO/ZnO/active layer/MoO$_3$/Al.

PBDB-T/IDT-OT [weight ratio]	V_{oc} [V]	J_{sc} [mA cm^{-2}]	FF [%]	PCE [%]	Thermal Annealing
1:0.8	0.868	7.21	47.5	2.97	160 °C, 10 min
1:1	0.927	8.27	43.4	3.32	160 °C, 10 min
1:1.5	0.867	5.10	48.6	2.15	160 °C, 10 min

Table S3 Photovoltaic performance of the PBDB-T/PC$_{71}$BM/IDT-OT ternary PSCs with different DIO content. The devices were in inverted structure of ITO/ZnO/active layer/MoO$_3$/Al.

PBDB-T/PC$_{71}$BM/IDT-OT [weight ratio]	V_{oc} [V]	J_{sc} [mA cm^{-2}]	FF [%]	PCE [%]	DIO [vol%]
1:1.5:0.2	0.891	12.98	62.3	7.26	0
1:1.5:0.2	0.870	14.89	66.45	8.61	0.2
1:1.5:0.2	0.869	15.35	68.1	9.09	0.5
1:1.5:0.2	0.850	14.23	68.9	8.34	1

Table S4 Photovoltaic properties of the binary PBDB-T/IDT-OT device with different annealing temperature under the optimal fabricated conditions.

Temperature [°C]	V_{oc} [V]	J_{sc} [mA cm^{-2}]	FF [%]	PCE [%]	Normalized PCE
r.t.	0.927	8.27	43.4	3.32	1
60	0.918	7.77	48.5	3.46	1.04
80	0.933	6.76	44.7	2.82	0.85
100	0.905	6.57	41.8	2.48	0.75
120	0.903	6.67	42.1	2.54	0.77
140	0.891	6.88	45.2	2.77	0.83
160	0.917	7.19	45.6	3.01	0.91

Table S5 Photovoltaic properties of the binary PBDB-T/PC$_{71}$BM device with different annealing temperature under the optimal fabricated conditions.

Temperature [°C]	V_{oc} [V]	J_{sc} [mA cm^{-2}]	FF [%]	PCE [%]	Normalized PCE
r.t.	0.826	14.10	66.8	7.78	1
60	0.831	11.99	69.5	6.92	0.89
80	0.854	12.98	66.9	7.41	0.95
100	0.851	11.58	67.5	6.65	0.85
120	0.836	11.15	64.0	5.97	0.77
140	0.845	11.48	67.3	6.53	0.84
160	0.852	10.43	68.2	6.06	0.78

Table S6 Photovoltaic properties of the ternary PBDB-T/PC$_{71}$BM/IDT-OT device with different annealing temperature under the optimal fabricated conditions.

Temperature [°C]	V_{oc} [V]	J_{sc} [mA cm^{-2}]	FF [%]	PCE [%]	Normalized PCE
r.t.	0.869	15.35	68.1	9.09	1
60	0.852	15.58	63.9	8.48	0.93
80	0.857	15.10	64.0	8.28	0.91
100	0.851	14.76	65.5	8.23	0.91
120	0.854	14.28	64.5	7.87	0.87
140	0.849	14.99	61.5	7.83	0.86
160	0.857	14.45	62.0	7.68	0.85

Table S7 Photovoltaic properties of the binary PBDB-T/IDT-OT device with different annealing time at 120 °C under the optimal fabricated conditions.

Annealing time [h]	V_{oc} [V]	J_{sc} [mA cm^{-2}]	FF [%]	PCE [%]	Normalized PCE
0	0.929	7.46	47.7	3.31	1
12	0.892	6.82	44.6	2.71	0.82
24	0.901	6.70	42.9	2.59	0.78
36	0.894	6.55	43.9	2.57	0.78
48	0.893	6.47	43.4	2.51	0.76
60	0.870	6.29	42.6	2.33	0.70

Table S8 Photovoltaic properties of the binary PBDB-T/PC$_{71}$BM device with different annealing time at 120 °C under the optimal fabricated conditions.

Annealing time [h]	V_{oc} [V]	J_{sc} [mA cm^{-2}]	FF [%]	PCE [%]	Normalized PCE
0	0.835	12.77	71.2	7.59	1
12	0.818	11.41	68.7	6.41	0.84
24	0.804	11.36	64.7	5.91	0.78
36	0.803	10.64	65.4	5.59	0.74
48	0.793	10.79	63.5	5.43	0.72
60	0.780	10.89	59.5	5.05	0.67

Table S9 Photovoltaic properties of the ternary PBDB-T/PC$_{71}$BM/IDT-OT device with different annealing time at 120 °C under the optimal fabricated conditions.

Annealing time [h]	V_{oc} [V]	J_{sc} [mA cm^{-2}]	FF [%]	PCE [%]	Normalized PCE
0	0.854	14.28	64.5	7.88	1
12	0.841	11.59	68.8	6.71	0.85
24	0.829	11.38	68.4	6.45	0.82
36	0.823	11.53	67.8	6.43	0.82
48	0.831	10.98	69.1	6.30	0.80
60	0.829	11.67	66.7	6.46	0.82

References

[1] W. Wang, B. Zhao, H. Wu, S. Liu, H. Liu, Z. Guo, W. Wei, C. Gao, *Dyes and Pigments* **2017**, *145* 345-353.